Journal of Low Temperature Physics, Vol. 95, Nos. 5/6, 1994

^{4}He on Weakly Attractive Substrates: Structure, Stability, and Wetting Behavior

B. E. Clements

Institute Laue Langevin, 38042 Grenoble Cedex, France

H. Forbert and E. Krotscheck

Department of Physics, Texas A & M University, College Station, TX 77843, USA

and

M. Saarela

Department of Theoretical Physics, University of Oulu, SF-90570 Oulu, Finland

(Received October 7, 1993; revised January 30, 1994)

Using a microscopic variational approach we examine the structure and the excitation spectrum of layered ^{4}He liquids absorbed to alkali metal and graphite substrates. We find that the alkali metal substrates produce a less pronounced layering structure than the shorter-range graphite/solid helium potential. For the excitations, three features are in common to the substrates: First, for coverages of a monolayer or more, a surface mode is present. Second, a bulk mode which gains strength as the coverage is increased, is identifiable for films with sufficiently high coverage. Finally, a two-dimensional mode that propagates within the first layer is observed for the more attractive substrates. We also present results that we obtain by using the nonlocal density functional theory. We document the reliability and shortcomings of this approach by making a detailed comparison of experimental, Monte Carlo, and variational theory results for the structure, energetics, and excitations. We also give a brief discussion on the wetting properties of helium on alkali metal and graphite/solid helium substrates.

1. INTRODUCTION

The structure, excitations, and growth of liquid ^{4}He films adsorbed to weakly attractive substrates is a matter of considerable experimental and theoretical research. It is an intriguing goal to uncover the underlying

0022-2291/94/0600-0849$07.00/0

mechanisms that drive an outwardly *simple-appearing* system to display a complicated growth scenario,[1,2] highly-complex neutron scattering spectra,[3,4] a multitude of thermodynamic phases,[5] transient superfluid behavior,[6] and so forth. From the point of view of the many-body theorist, this is an ideal system because each of above characteristics is a direct consequence of many-body correlations inherent to a hard-core boson liquid in a confined geometry.

In this work we extend our previous investigation of boson quantum film structures[7] and dynamics,[8,9] based on variational hypernetted chain/Euler-Lagrange (HNC/EL) theory and generalized linear-response theory, to address three important issues:

First, we have broadened our set of substrate potentials to include the alkali metals: magnesium, lithium, and sodium. These substrates differ from the solid helium on graphite potential, studied by us earlier, because they tend to be longer range and, with the exception of Mg, they have substantially shallower well depths. An intriguing reason for studying such long-range, shallow potentials is the prospect of using the HNC/EL theory to observe behavior that differs qualitatively from the solid helium/graphite potential. For example, for Na, the weakest substrate potential studied here, we do *not* find a solution to our HNC/EL equations which corresponds to a uniform monolayer covering. This behavior is unlike that of the other substrates where we always observe a stable monolayer structure when the coverage exceeds the spinodal point coverage for the formation of two-dimensional clusters. This observation implies that, in the early stages of the growth of the helium film on a Na substrate, the helium atoms form bulk-like clusters, several atoms thick in the dimension perpendicular to the substrate. A certain coverage (near that of a double layer) must be reached before the helium clusters fully connect to uniformly cover the surface.

Our second purpose for this work is to carry out a detailed comparison of experimental, Monte Carlo, and HNC/EL results, with those obtained from currently-used forms of density functional theory. In practice the form of density functional theory most commonly employed to investigate quantum film structures is the nonlocal density functional theory (NLDFT) developed mainly by Treiner and collaborators.[10,11] To make our comparison complete, we have generated the structure and energetics produced by NLDFT for the two- and three-dimensional limits, and for the case of the quantum films. We also give a brief discussion on the wetting properties of helium on the graphite and alkali metal substrates; we argue that the wetting phenomenon is not a stringent test for a many-body theory.

While NLDFT is perhaps the most successful form of density functional theories used for quantum films, our analysis shows that it has

several severe shortcomings. We defer a more complete discussion until Sec. 4, but it is worthwhile to point out from the start the root problem with NLDFT (and similar theories) which causes these theories often to miss very fundamental physics. A descriptive discussion suffices to illustrate the point.

A thoroughly studied criterion, that good many-body theories must satisfy, is that long- and short-range correlations must be treated in a symmetric way. The basic premise, which is conventionally stated in standard perturbation theories, such as parquet theory, is that to insure the proper long- and short-range screening, long-range interactions must drive the integral equations that generate the short-range interactions and vice versa. This statement stems from the important work of Baym and Kadanoff[12] and Parquet theory.[13] We note that HNC/EL theories fit into that category; the work by Jackson, Lande and Smith[14] shows that HNC/EL theories consistently sum ladder (short-range) and ring (long-range) diagrams, for a given local approximation to the total scattering amplitude. In contrast, it is obvious that theories such as NLDFT which derive a one-body Euler equation from the energy functional but drive it with an effective Hartree potential that is fitted from uniform-bulk data can no longer ensure this consistency. This shortcoming can most noticeably lead to incorrect predictions when the short-range structure or the stability of the system is in question.

Our final goal is to examine the low-lying excitations that could be observed in future neutron scattering experiments. This goal is achieved in Sec. 6 where, at the level of the Feynman theory of excitations, we calculate the dynamic structure function and the transition densities. We extend our comparison of HNC/EL theory and NLDFT to include the excitations by calculating the particle-hole interaction consistent with the NLDFT density functional and from that the dynamic structure function within that theory.

2. MICROSCOPIC THEORY

Quantitatively the most successful microscopic theories for strongly-interacting quantum liquids are based on a variational *ansatz* for the ground-state wave function of the many-body system of the Jastrow-Feenberg form

$$\Psi_0(\mathbf{r}_1, \ldots, \mathbf{r}_N) = \exp \tfrac{1}{2}\left[\sum_i u_1(\mathbf{r}_i) + \sum_{i<j} u_2(\mathbf{r}_i, \mathbf{r}_j) + \sum_{i<j<k} u_3(\mathbf{r}_i, \mathbf{r}_j, \mathbf{r}_k)\right] \quad (2.1)$$

The only phenomenological input to the theory is the microscopic Hamiltonian which we assume to be of the form

$$H=\sum_i\left[-\frac{\hbar^2}{2m}\nabla_i^2+U_{\text{sub}}(\mathbf{r}_i)\right]+\sum_{i<j}V(|\mathbf{r}_i-\mathbf{r}_j|) \tag{2.2}$$

where $V(|\mathbf{r}_i-\mathbf{r}_j|)$ is the liquid ^{4}He-^{4}He interaction, and $U_{\text{sub}}(\mathbf{r})$ is the substrate-adsorbate potential. The only other approximations occur because of the choice to restrict the wave function (2.1) to triplet correlations and because of the effort one is willing to spend in the computation of the relevant "elementary" diagrams. An important part for the approach is the optimization of the many-body correlations by solving the Euler equations

$$\frac{\delta E}{\delta u_n(\mathbf{r}_1,\ldots,\mathbf{r}_n)}=0 \tag{2.3}$$

where E is the energy expectation value of the Hamiltonian (2.2) with respect to the wave function (2.1).

In order to describe our procedure and results, we must briefly review the basic ingredients of the theory. We keep this description to the bare essentials. The derivation of the basic formalism may be found in Ref. 15; the most recent implementation of the formalism and details on our treatment of triplet correlations are found in Ref. 7. The theory is the generalization of the homogeneous-phase theory which reproduces the equation of state, pair distribution functions, and structure functions in both two and three dimensions with excellent accuracy.[16] In the computationally more demanding case of non-uniform liquids, a few numerical compromises are necessary which cause a somewhat reduced accuracy. We discuss this below. It is important to point out that the identical equations can be derived, within the parquet-diagram theory, without ever mentioning the Jastrow-Feenberg wave function. However, the formulation in terms of such a variational problem is useful because direct contact to Monte Carlo calculations is then possible.

As a first step of the theory, the energy expectation value is rewritten as a functional of the physically observable one-body density $\rho_1(\mathbf{r})$ and the pair distribution function $g(\mathbf{r},\mathbf{r}')$. This task is accomplished by using the Born-Green-Yvon equation for the one-body density, and the hypernetted chain equation for the pair distribution function. A natural representation of the resulting energy expectation value is

$$E=\int d^3r\left[\frac{\hbar^2}{2m}|\nabla\sqrt{\rho_1(\mathbf{r})}|^2+\rho_1(\mathbf{r})\,U_{\text{sub}}(\mathbf{r})\right]+E_c[g(\mathbf{r},\mathbf{r}'),\rho_1(\mathbf{r})] \tag{2.4}$$

where E_c is the "correlation energy." It's precise functional form is irrelevant for the purpose of our present discussion, the only important feature of this "correlation energy functional" is that variational derivatives with respect to the one-body density *and* the pair distribution function are well defined and can be calculated within reasonable computational effort.

The energy functional is then minimized with respect to the one-body density, which leads to a generalized Hartree-equation

$$\left[-\frac{\hbar^2}{2m}\nabla^2 + U_{\text{sub}}(\mathbf{r}) + V_H(\mathbf{r}) \right] \sqrt{\rho_1(\mathbf{r})} = \mu \sqrt{\rho_1(\mathbf{r})} \tag{2.5}$$

where $V_H(\mathbf{r}) \equiv \delta E_c / \delta \rho(\mathbf{r})$, and μ is the chemical potential.

The minimization of the energy with respect to the pair distribution function $g(\mathbf{r}, \mathbf{r}')$ gives rise to a second, two-body Euler equation,

$$\frac{\delta E_c}{\delta g(\mathbf{r}, \mathbf{r}')} = 0 \tag{2.6}$$

and the combined set of equations, i.e., the energy expression (2.4), the one- and two-body equations (2.5) and (2.6), and a corresponding equation for the triplet correlation function u_3,[7] are referred to as hypernetted chain/Euler-Lagrange (HNC/EL) equations. A useful formulation of the two-body equation is the form of a generalized eigenvalue problem

$$\int d^3r' [\delta(\mathbf{r} - \mathbf{r}') H_1(\mathbf{r}) + 2\tilde{V}_{\text{p-h}}(\mathbf{r}, \mathbf{r}')] H_1(\mathbf{r}') \psi_\omega(\mathbf{r}') = (\hbar\omega)^2 \psi_\omega(\mathbf{r}) \tag{2.7}$$

where

$$\begin{aligned} H_1(\mathbf{r}) &\equiv -\frac{\hbar^2}{2m} \frac{1}{\sqrt{\rho_1(\mathbf{r})}} \nabla\rho_1(\mathbf{r}) \cdot \nabla \frac{1}{\sqrt{\rho_1(\mathbf{r})}} \\ &= -\frac{\hbar^2}{2m}\nabla^2 + U_{\text{sub}}(\mathbf{r}) + V_H(\mathbf{r}) - \mu \end{aligned} \tag{2.8}$$

is an effective one-body Hamiltonian, and $\tilde{V}_{\text{p-h}}(\mathbf{r}, \mathbf{r}')$ is the so-called "particle-hole interaction" which can, in turn, be expressed in closed form as a functional of the bare two-body interaction, the one-body density, and the pair distribution function. Normalizing the eigen-states of Eq. (2.7) as

$$(\psi_\omega | H_1 | \psi_{\omega'}) = \hbar\omega \delta_{\omega\omega'} \tag{2.9}$$

and defining the adjoint states

$$\phi_\omega(\mathbf{r}) = \frac{1}{\hbar\omega} H_1 \psi_\omega(\mathbf{r}) \tag{2.10}$$

allows the pair distribution function to be represented in a normal-mode decomposition

$$g(\mathbf{r}, \mathbf{r}') - 1 = \sum_{\omega} \psi_{\omega}(\mathbf{r})\, \psi_{\omega}(\mathbf{r}') - \delta(\mathbf{r} - \mathbf{r}'). \tag{2.11}$$

The pair distribution function obtained in this manner can then be used to re-calculate the one-body effective potential $V_H(\mathbf{r})$ and the particle-hole interaction $V_{\text{p-h}}(\mathbf{r}, \mathbf{r}')$. The eigenvalue problem (2.7) is then solved again with these updated functions, and the process is repeated until convergence is reached. A necessary condition for the existence of solutions of the two-body Euler equation is that all eigenvalues $\hbar^2\omega^2$ are positive. In fact, the two-body Euler equation (2.7) is nothing but a reformulation of the random phase approximation (RPA) for the density-density response function,[17] and the eigenvalues of Eq. (2.7) are identical to the poles of the density-density response function. The condition that all eigenvalues of Eq. (2.7) must be positive is, in the language of linear response theory, nothing else but the condition that the physical system should be stable against infinitesimal density fluctuations.

An important alternative definition of $\tilde{V}_{\text{p-h}}(\mathbf{r}, \mathbf{r}')$ is

$$\tilde{V}_{\text{p-h}}(\mathbf{r}, \mathbf{r}') = \sqrt{\rho_1(\mathbf{r})}\, \frac{\delta^2 E_c}{\delta\rho_1(\mathbf{r})\, \delta\rho_1(\mathbf{r}')}\, \sqrt{\rho_1(\mathbf{r}')}. \tag{2.12}$$

However, the particle-hole interaction obtained from the *first variation with respect to the pair correlation function*, and the one obtained from the *second variation with respect to the one-body density* will agree only in an exact evaluation and optimization of all ground-state quantities.

3. DENSITY FUNCTIONAL THEORY

When the energy is written in the form (2.4) and supplemented by the two-body Euler equation determining the pair-distribution function $g(\mathbf{r}, \mathbf{r}')$, one can think of the variational theory as a version of density functional theory with a very specific, non-local energy functional. However, conventionally density functional theory bypasses the step of deriving the energy from two-body (and higher) correlation functions, or by the summation of Feynman diagrams and resorts to using phenomenological or heuristic input to formulate an energy functional that can be varied with respect to density to yield a Hartree-equation (2.5). The significant technical simplification of such a step is that it eliminates the need to solve a two-body equation. Moreover, one has the freedom to use known information on the features of the macroscopic many-particle system. An important drawback

of this simplification is that the theory can, and will normally have, unphysical solutions which are unstable against infinitesimal density fluctuations.

The most popular density functional theory is the *local density approximation* which assumes that the correlation energy of the system can be approximated as the integral over the local energy density of the *homogeneous* system, i.e.

$$E_c = \int d^3r\, \varepsilon_c[\rho(\mathbf{r})] \tag{3.1}$$

where $\varepsilon_c(\rho)$ is the energy density of the bulk system at the density ρ. Local density functional theory has been applied by Ji and Wortis[18] to examine the properties of adsorbed helium films.

One problem of a local density functional is that, when such a functional is fitted to the bulk equation of state in the experimentally accessible regime, the experimental surface energy is not well reproduced. A second problem occurs when one studies atomic monolayers: If one compresses the liquid such that it becomes "almost" two-dimensional, the density approaches the form

$$\rho(\mathbf{r}) \approx \rho_{2D}\,\delta(z). \tag{3.2}$$

In that limit, *any* energy functional of the local density which contains terms of the form $\rho^\alpha(\mathbf{r})$ with $\alpha > 1$ diverges. While it is not *a priori* clear that the density distribution of an atomic monolayer is "close enough" to a δ-function for this divergence to be relevant, it is the matter of a very simple numerical calculation to verify that the energetics of a realistic atomic monolayer would, in the LDA, indeed be dominated by the spurious divergence of the energy functional. One of the problems of the LDA, i.e. the poor prediction of the surface energy, can be corrected by adding a gradient correction term, for example by using an energy functional of the form

$$\varepsilon_c[\rho, \nabla\rho] = \varepsilon_c(\rho) + d\,|\nabla\rho|^2. \tag{3.3}$$

This generalization introduces an additional free parameter, d, which can be adjusted such that the surface energy is reproduced. However, more than what is gained in one aspect is lost in others: The divergence of the energy functional in the two-dimensional limit discussed above is made worse. Moreover, the gradient-corrections induce a large anomalous dispersion of the zero-sound spectrum in the homogeneous, three-dimensional liquid. Consequently, even for low energies, the zero-sound spectrum has little resemblance to reality.

A further problem with both density functionals discussed above is that they lack any hard-core structure. As a consequence, none of the layer structure that is well established for adsorbed liquids,[19] and quantum liquid clusters,[20] is predicted by these theories. We conclude that local density functional theories (or non-local with gradient corrections) miss much of the important physics of non-uniform quantum liquids; we shall therefore, not discuss such theories any further.

In an attempt to overcome the hard-core problem, Pavloff and Treiner[10] introduced a non-local energy functional of the form

$$E_c = \frac{1}{2}\int d^3r_1\, d^3r_2\, \rho(\mathbf{r}_1)\, \rho_1(\mathbf{r}_2)\, V_l(|\mathbf{r}_1 - \mathbf{r}_2|) + \frac{c_{3D}}{2}\int d^3r\, \rho(\mathbf{r})\, \bar{\rho}^{1+\gamma}(\mathbf{r}) \quad (3.4)$$

where $V_l(r)$ is a "screened" potential, which is derived from the Lennard-Jones interaction:

$$V_l(r) = \begin{cases} 4\varepsilon\left[\left(\dfrac{\sigma}{r}\right)^{12} - \left(\dfrac{\sigma}{r}\right)^{6}\right] & \text{for} \quad r \geqslant h \\ V_l(h)\left(\dfrac{r}{h}\right)^4 & \text{for} \quad r < h \end{cases} \quad (3.5)$$

with the de Boer-Michel parameters $\varepsilon = 10.22$ K and $\sigma = 2.556$ Å, and

$$\bar{\rho}(\mathbf{r}) = \int d^3r'\, n_{3D}(\mathbf{r} - \mathbf{r}')\, \rho(\mathbf{r}') \quad (3.6)$$

where

$$n_{3D}(\mathbf{r}) = \frac{3}{4\pi h^3}\,\theta(h - |\mathbf{r} - \mathbf{r}'|) \quad (3.7)$$

is a normalized 3-D sphere. We will refer to the above form of the energy as to the Orsay-Paris energy functional.

The energy functional (3.4) removes the most imminent problems of local density functional theories: The core-repulsion of the screened interaction, $V_l(r)$, is still strong enough to generate a layer structure of adsorbed films,[21] the two-dimensional limit of the correlation energy is finite, the surface energy is in reasonable agreement with experiments, and the zero-sound dispersion relation is also within reasonable bounds of what one would expect. With the worst *qualitative* shortcomings of the local density functional theory removed, the remaining open question is to what extent the theory is capable of making *quantitative* predictions for properties that have not been used to determine the parameters h, c_{3D}, and γ of the energy

functional. Since we are interested in the behavior of liquid films in the full regime between an (almost two-dimensional) liquid sub-monolayer and the three-dimensional limit, comparisons must be made for both the two- and the three-dimensional homogeneous liquids for which experimental[22] and Monte Carlo[23,24] results are available, and for the layered-film structures in the intermediate regime.

4. ENERGETICS AND STRUCTURE IN TWO AND THREE DIMENSIONS

We expand in this chapter upon a recent analysis of the energetics of the two- and three-dimensional homogeneous ^{4}He phases[7] by presenting also results for the chemical potentials and structure functions obtained from the nonlocal density functional theory (NLDFT). Comparison of these results with experimental and/or Monte Carlo data provide the clearest assessment of predictive power of the density functional approach.

In the limit of a homogeneous, three-dimensional liquid, the energy functional (3.4) assumes the form

$$\frac{E_c^{3D}}{N} = \frac{b_{3D}}{2}\rho_{3D} + \frac{c_{3D}}{2}\rho_{3D}^{1+\gamma} \tag{4.1}$$

where N is the particle number, and $b_{3D} = \int d^3r\, V_l(r)$. The parameters c_{3D} and γ are identical to those used in the density functional of Ref. 25, and the cutoff parameter h is chosen such that the coefficient b_{3D} also matches the corresponding value of Ref. 25. By construction, the energy per particle given by this parameterization agrees with the experimental equation of state.

The two-dimensional limit of the theory is obtained by assuming a density of the form (3.2). One then obtains again an equation of state of the form

$$\frac{E_c^{2D}}{N} = \frac{b_{2D}}{2}\rho_{2D} + \frac{c_{2D}}{2}\rho_{2D}^{1+\gamma} \tag{4.2}$$

with $b_{2D} = \int d^2r\, V_l(r)$ and $c_{2D} \equiv c_{3D}(3/4h)^{1+\gamma}$.

In the three-dimensional case, the equations of state obtained from experiments,[22] calculated by Monte Carlo[23] or variational theory,[16,7] or fitted by the parameterization of the density functional (4.1)[25] are practically indistinguishable. This is no longer true in the two-dimensional limit, where the results of our variational theory still agree very well with Monte Carlo data, but the non-local density functional predicts an energy per particle (4.2) that is significantly too high, c.f. Fig. 1.

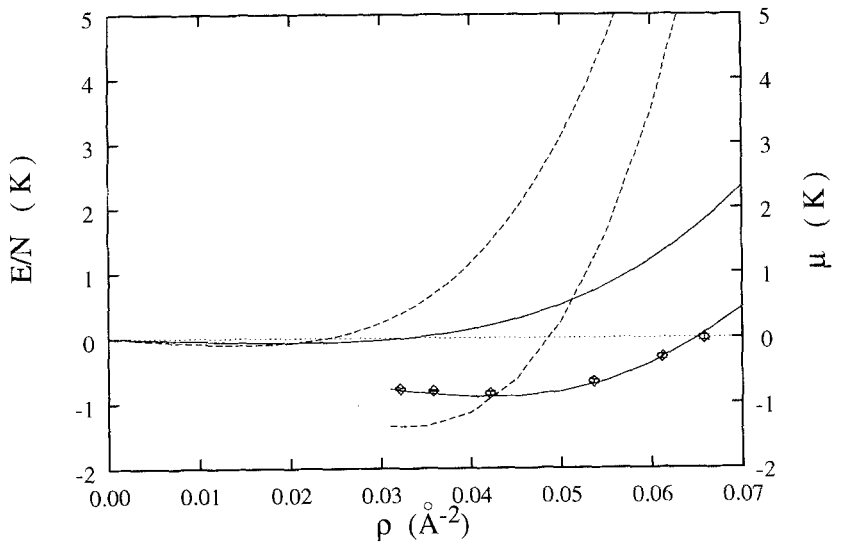

Fig. 1. The energy per particle (solid lines) and the chemical potential (dashed lines) of two-dimensional ^{4}He are shown as obtained within the HNC/EL theory (Ref. 7 lowest two lines) and density-functional theory (Ref. 10, upper two lines). Also shown are the Green's functions Monte Carlo data (Ref. 24, diamonds with error bars).

Even though the "correlation energy" E_c is, in the realistic situation of an atomic monolayer adsorbed to a substrate, normally small compared with the binding energy of a single particle to the substrate, the difference between the equations of state has significant consequences on the phase-diagram of a liquid monolayer of ^{4}He atoms on a substrate: Both Monte Carlo and variational calculations predict that the two-dimensional phase is a *liquid* at low temperatures. The energy per particle has a minimum at a surface coverage of about 0.04 atoms/Å^2. Below that surface coverage, the surface would be covered (at finite temperatures) by a liquid-gas coexistence phase, and at zero temperature by two-dimensional liquid clusters.

This conclusion is consistent with Greywall's phase diagram of ^{4}He adsorbed to graphite.[5] The Orsay-Paris energy functional can lead to a *qualitatively different* scenario: The 2D system is only insignificantly bound, with a maximum binding energy of about -0.06 K at a very low density $\rho_{2D}^{\min} \approx 0.02$ atoms/Å^2. Therefore one would conclude that above the temperature of about 0.06 K the two-dimensional system is a gas, and would spread out uniformly over the surface of the substrate. The same holds true for atomic monolayers in a sufficiently strong external holding potential.

The calculation of the excitation spectrum and the static structure function is an integral part of the HNC/EL theory. To calculate the same quantities within the density functional method,[11] one starts from the definition (2.12) of the particle-hole interaction. Carrying out the second variation, one obtains

$$V_{\text{p-h}}(\mathbf{r}, \mathbf{r}') = V_l(|\mathbf{r}-\mathbf{r}'|) + \frac{c_{3D}(1+\gamma)}{2}\left[\bar{\rho}^{\gamma}(\mathbf{r}) + \bar{\rho}^{\gamma}(\mathbf{r}')\right] n_{3D}(|\mathbf{r}-\mathbf{r}'|) + \frac{c_{3D}\gamma(1+\gamma)}{2}\int d^3r''\, \rho(\mathbf{r}'')\, \bar{\rho}^{\gamma-1}(\mathbf{r}'')\, n_{3D}(|\mathbf{r}-\mathbf{r}''|)\, n_{3D}(|\mathbf{r}'-\mathbf{r}''|) \tag{4.3}$$

In both cases of the uniform liquid, the particle-hole interaction is translationally invariant. The Fourier transform in $n=2$ or $n=3$ dimensions gives

$$\tilde{V}^{nD}_{\text{p-h}}(q) \equiv \rho_{nD}\int d^n r\, V_{\text{p-h}}(r)\, e^{i\mathbf{q}\cdot\mathbf{r}} = \rho_{nD}\int d^n r\, V_l(r)\, e^{i\mathbf{q}\cdot\mathbf{r}} + (1+\gamma)\, c_{nD}\rho_{nD}^{1+\gamma}\left[l_n(hq) + \frac{\gamma}{2} l_n^2(hq)\right] \tag{4.4}$$

where

$$l_n(x) = \begin{cases} \dfrac{3}{x} j_1(x) & \text{for} \quad n=3 \\ \dfrac{2}{x} J_1(x) & \text{for} \quad n=2 \end{cases} \tag{4.5}$$

With these particle-hole interactions, one can solve Eq. (2.7) in momentum space for the excitation spectrum

$$\hbar\omega(q) = \frac{\hbar^2 q^2}{2m}\left[1 + \frac{4m\tilde{V}^{nD}_{\text{p-h}}(q)}{\hbar^2 q^2}\right]^{1/2} \tag{4.6}$$

and obtain the static structure function in two and three dimensions by the usual Bogoliubov theory,

$$S(q) = \left[1 + \frac{4m\tilde{V}^{nD}_{\text{p-h}}(q)}{\hbar^2 q^2}\right]^{-1/2} \tag{4.7}$$

Of course, it is noted that the excitation spectrum is, in this approximation, the Feynman spectrum with its well-known shortcomings. However, the Feynman theory of excitations is the necessary first step in any attempt to improve upon the description of the excitations, either by correlated-basis-functions theory[26] or by allowing for time-dependent pair-correlations.[27,28]

Figures 2 and 3 show a comparison between HNC/EL, density functional, and experimental/Monte Carlo results for a sequence of densities. The comparison between HNC/EL and experimental/Monte Carlo data has been discussed in Ref. 7, it is sufficient here to concentrate on the discussion of the density functional results. In three dimensions, the height of the peaks of $S(q)$ in the NLDFT and the HNC/EL results agree quite well with the data by Svensson,[29] whereas those of Robkoff and Hallock[30] are slightly higher. The wavelength of the oscillations of $S(q)$ for larger momenta is, however, somewhat longer than experimentally found; this indicates that the density functional theory does not correctly describe the hard core structure of the pair distribution function. Such a feature, which relies heavily on a self-consistent description of both short- and long-range correlations, is certainly also not expected from a simple RPA like theory with an effective interaction.

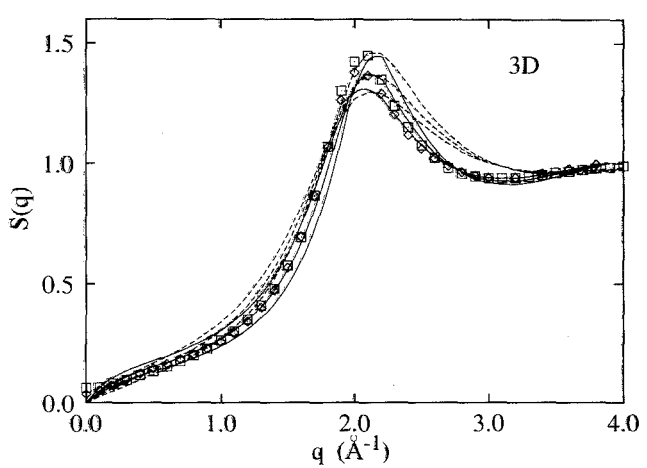

Fig. 2. The static structure function of the three-dimensional homogeneous liquid is compared, for densities $\rho_{3D} = 0.020$, 0.022, and 0.024 Å^{-3}, between HNC/EL (solid lines) and NLDFT (dashed lines). Also shown are experimental data by Svensson *et al.* (Ref. 29, diamonds) and Robkoff *et al.* (Ref. 30, boxes) at the saturation vapor pressure. The functions with the highest peak correspond to those with the highest density.

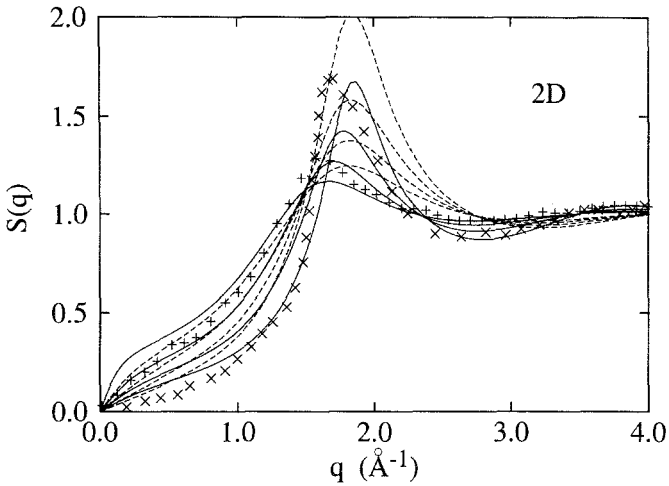

Fig. 3. The static structure function of the two-dimensional homogeneous liquid is compared, for densities $\rho_{2D} = 0.035$, 0.045, 0.055, and 0.065 Å^{-2}, between HNC/EL (solid lines) and NLDFT (dashed lines). The functions with the highest peak correspond to those with the highest density. Also shown are Monte Carlo results,[24] for $\rho_{2D} = 0.0421$ Å^{-2} which is near equilibrium (+-symbols) and $\rho_{2D} = 0.0658$ Å^{-2} (×-symbols) which is a density just before freezing.

The situation changes rather dramatically when we turn to the two-dimensional case (Fig. 3): There the Monte Carlo and the HNC/EL structure functions agree quite well, except for a small shift of the peak at very high densities. The structure functions obtained by the density functional theory, on the other hand, display consistently a peak that is too high, and oscillations that are too long. The structure functions resemble those of a much denser system. This is consistent with the observation that the pressure determined by NLDFT for densities in the range 0.035 Å^{-2} to 0.065 Å^{-2} (Fig. 1) would indicate that the system is at a considerably higher pressure than that which is predicted by Monte Carlo or the variational theory.

5. QUANTUM LIQUID FILM ENERGETICS

In HNC/EL theory, one always solves the two-body equation simultaneously with the one-body equation, but in the NLDFT, there is no *a priori* need to introduce two-body quantities. In *both* methods, the properties of excited states can be examined by solving Eq. (2.7); the NLDFT using the definition (2.12) for the particle-hole interaction. Examining the long-wavelength properties of the excitation functions, one

can then also determine whether a given background solution is locally stable or not. In particular, the long-wavelength limit of the excitation energy can be calculated in closed form from the eigenvalue problem (2.7). The eigenvalue Eq. (2.7) can be decoupled in momentum space as a function of the momentum $q_{||}$ parallel to the surface. The long-wavelength limit of the lowest-lying mode, which we identify with the third sound, can be calculated and is found to be

$$\hbar\omega_3(q_{||}) = \hbar c_3 q_{||} \tag{5.1}$$

with

$$mc_3^2 = \frac{\hbar^2}{2m} \frac{n}{(\sqrt{\rho}\,|[H_1(0) + 2\tilde{V}_{\text{p-h}}(0)]^{-1}|\,\sqrt{\rho})} \tag{5.2}$$

where $n = \int dz\, \rho_1(z)$ is surface coverage, and $H_1(0)$ and $\tilde{V}_{\text{p-h}}(0)$ are the long-wavelength limits of the corresponding quantities defined above. The relationship (5.2) may also be derived from Eq. (2.5); one finds the well-known hydrodynamic relationship

$$mc_3^2 = n \frac{d\mu}{dn}. \tag{5.3}$$

In the NLDFT, the definitions (5.3) and (5.2) are rigorously identical. In the HNC/EL theory, the same precautions as mentioned above apply: The speed of third sound calculated by the hydrodynamic derivative (5.3) and the long-wavelength limit of the collective excitations, Eq. (5.2) will normally agree only for an exact theory. In general, one expects that the expression (5.2) is less accurate than the hydrodynamic derivative (5.3) since the diagrams included in Eq. (5.2) are a proper subset of those included in Eq. (5.3). In particular for thick films, where the third sound velocity goes to zero, one must expect large-scale numerical cancellation in the evaluation of expression (5.2).

For comparison between the predictions of density functional theory and the HNC/EL theory, we have chosen four different substrate potentials. One of these potentials, which we have studied at some length earlier,[7] is a simple model of two layers of solid helium on graphite. The substrate potential consists of three terms,

$$U_{\text{sub}}(z) = U_0(z + z_0) + \sum_{i=1}^{2} U_i(z + z_i) \tag{5.4}$$

with

$$U_0(z) = e\left[\frac{1}{15}\left(\frac{\sigma}{z}\right)^9 - \frac{1}{2}\left(\frac{\sigma}{z}\right)^3\right] \tag{5.5}$$

where the strength e is chosen to match the asymptotic strength of the graphite-helium interaction,[31] $e\sigma^2/2 = 186$ meV. The two solid helium planes are modeled by averaging Lennard-Jones potentials over a plane,

$$U_i(z) = 4\pi\varepsilon n_i \sigma^2 \left[\frac{1}{5}\left(\frac{\sigma}{z}\right)^{10} - \frac{1}{2}\left(\frac{\sigma}{z}\right)^4 \right] \tag{5.6}$$

with $\varepsilon = 10.22$ K and $\sigma = 2.556$ Å. The surface densities n_i $(i = 1, 2)$ were taken to be the experimental values[3] $n_1 = 0.115$ Å^{-2} and $n_2 = 0.093$ Å^{-2}. The offsets z_i are such that the distance between individual solid layers and between the first solid layer and the substrate is about 3.3 Å. The model is undoubtedly somewhat crude; it leaves out, along with any surface corrugation, a number of important many-body effects. A somewhat more extensive discussion, and an examination of the dependence of our quantum film structures on the strength of the substrate potential is found in Ref. 7.

A second, somewhat simpler family of substrate potentials has been used in density functional calculations in an attempt to explain the wetting behavior of ^{4}He on alkali metal substrates.[21] These potentials are 3–9 potentials characterized by their *range* C_3 and their *well depth* D. They have the analytic form

$$U_{\text{sub}}(z) = \left[\frac{4C_3^3}{27D^2} \right] \frac{1}{z^9} - \frac{C_3}{z^3}. \tag{5.7}$$

Fig. 4 provides a comparison of these four different potentials. It is seen that they span a somewhat broader set than those we studied in our previous work. In particular, the "solid helium" potential is of considerably shorter range, whereas the magnesium substrate has the deepest potential well.

The structure and energetics predicted for liquid films by the microscopic HNC/EL theory has been discussed at length in Ref. 7, it is sufficient here to review our results. It was already pointed out that the HNC/EL equations have no solution if the system is unstable against infinitesimal density fluctuations. This is particularly relevant for the energetics of the growth of helium films on the solid helium substrate. At very low densities the first liquid layer of atoms (we will refer to this layer as to the "first" layer, independently of whether the substrate itself consists of solid ^{4}He layers) will form a low-density two-dimensional liquid. The saturation density of this liquid, ρ_{2D}, is known[24] to be approximately 0.043 Å^{-2}. As long as the substrate potential is sufficiently deep and narrow such that the degree of freedom to move in the z direction is, for all practical purposes, "frozen out," this coverage should be essentially independent of the strength

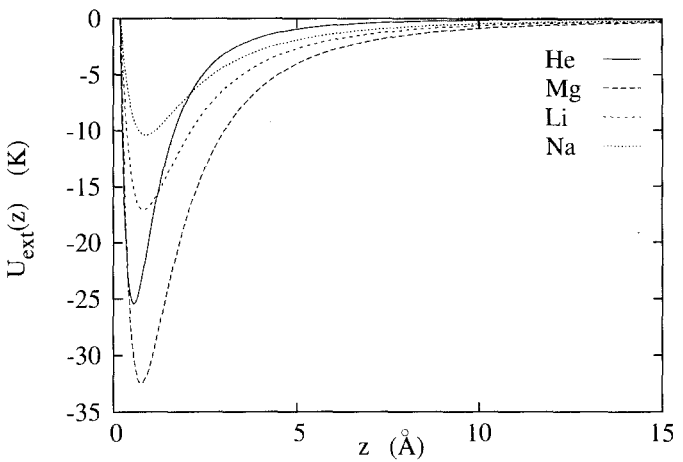

Fig. 4. A comparison of the substrate potentials defining the graphite/solid helium model (solid line), and the Mg (long-dashed line), Li (short-dashed line) and Na (dotted line) substrates. The parametrization of the alkali metal potentials is taken from Ref. 21.

of the substrate potential. In fact, Greywall[5] finds that even the *first* monolayer on graphite is in a liquid/gas (or, at $T=0$, liquid-vacuum) coexistence regime below a coverage of $n=0.04$ Å^{-2}. This is in excellent agreement with what one would expect, from Monte Carlo calculations and our HNC/EL results, for the stable coverage of a two-dimensional system. Below a certain minimum density of about $\rho_{2D_{\min}} \approx 0.037$ the compressibility vanishes and the two-dimensional system becomes unstable against infinitesimal density fluctuations. It is important to note that ρ_{2D} is considerably below the saturation density, ρ_{3D}, of three-dimensional ^{4}He, which would translate into a surface density of $\rho_{3D}^{2/3} \approx 0.077$ Å^{-2}. Therefore, by adding further atoms to the liquid, the two-dimensional system must become highly compressed in order to approach the bulk equilibrium density. While a weakly attractive adsorbate-substrate interaction would naturally favor a compressed layer, a density will inevitably be reached at which point it becomes energetically favorable to elevate particles to a second (or even a third) layer, before the first layer can be further compressed. To what extent such a behavior is repeated depends on both the strength and the range of the substrate potential. In Ref. 7, we have found at least two more such layering transitions. These transitions could provide an interpretation of the "re-entrant superfluidity" found recently in torsional oscillator experiments.[6]

The scenario described above is most easily discussed by considering the coverage dependence of the chemical potential and the long-wavelength

limit of the (third) sound velocity, which is conveniently expressed as mc_3^2. As a unique feature of the HNC/EL theory, we have found in Ref. 7 that the chemical potential of a ^{4}He atom on the graphite/solid helium substrate is *not* a monotonic function, and that the sound velocity of the homogeneous phase can become imaginary. In that situation, the HNC/EL equations have no solutions unless one projects out the very long-range excitations. A further prediction of our analysis is that, for low coverages, the chemical potential should be essentially equal to the binding energy e_0 of a single particle to the substrate, *plus* the chemical potential of the *two-dimensional* liquid, $\mu_{2D}(n)$,

$$\mu(n) \approx e_0 + \mu_{2D}(n) \tag{5.8}$$

Fig. 5 shows the coverage dependence of the chemical potential obtained from both the HNC/EL calculation and the NLDFT. Indeed, for the monolayer, the chemical potential follows quite closely the estimate from (5.8); the fact that the chemical potential of the films is somewhat lower is because of the additional degree of freedom of moving in the z direction. The comparison with the NLDFT shows basically the same picture. Of course, there the chemical potential has been calculated consistently in NLDFT. The behavior of the film deviates much earlier from the two-dimensional behavior, which is also plausible since in NLDFT that geometry appears to be energetically unfavorable to the particles.

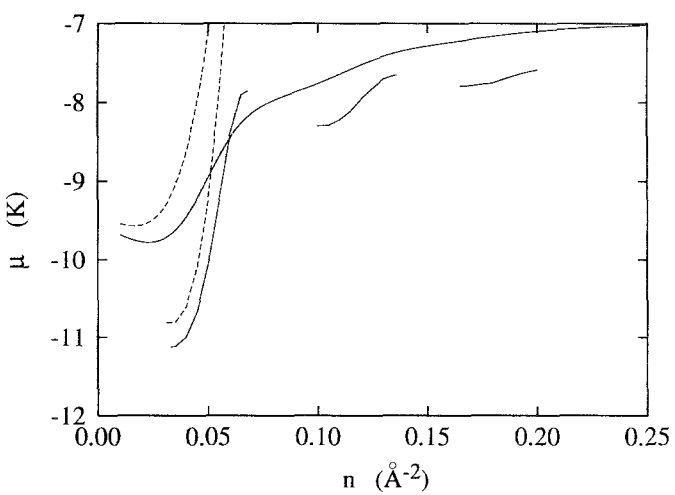

Fig. 5. The chemical potential of ^{4}He films adsorbed to the graphite/solid helium substrate is shown as obtained from the HNC/EL theory (lower fragmented solid lines) and NLDFT (upper solid line). Also shown are the estimates of Eq. (5.8) in HNC/EL (lower dashed line) and NLDFT (upper dashed line) for the monolayer.

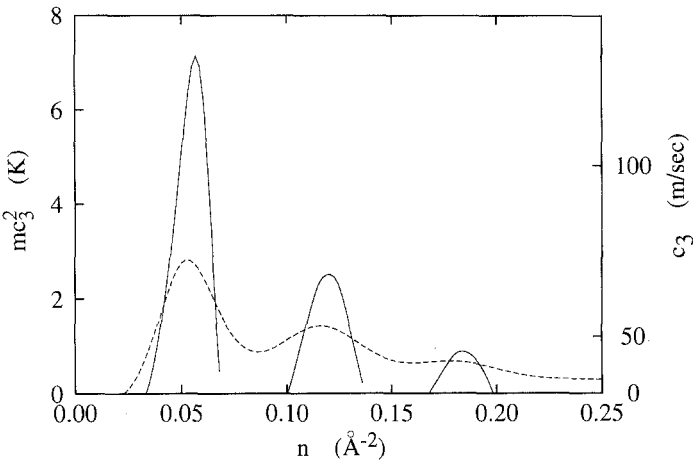

Fig. 6. The (square of) the speed of sound, mc_3^2 (left scale) and c_3 (right scale) of ^{4}He films adsorbed to the graphite/solid helium substrate is shown as obtained from the HNC/EL theory (solid line) and NLDFT (dashed line).

The comparison of the sound velocities as a function of coverage in Fig. 6, and the density profiles in Fig. 7 show basically the same picture. In the NLDFT, two-dimensional layers appear to be energetically less favorable. Particles are pushed out of the layers at a lower coverage, and the coverage dependence of the sound velocity becomes smoother. While

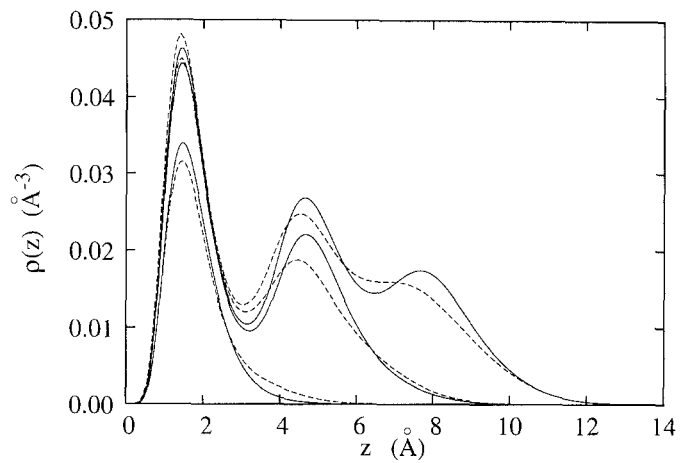

Fig. 7. The density profiles of ^{4}He films adsorbed to the graphite/solid helium substrate is shown as obtained from the HNC/EL theory (solid lines) and NLDFT (dashed line). The three curves correspond to coverages of $n = 0.05$ Å^{-2}, $n = 0.12$ Å^{-2}, and $n = 0.18$ Å^{-2}.

the layering transitions appear to be intrinsic properties of the comparably short-ranged substrate potential, and are shown to be stable against variations of the potential strength, we hesitate to attribute too much significance to the magnitude of the sound velocity. We have shown in Ref. 7 that the sound velocity is a sensitive function of the potential strength, and a change of the attractive portion by 10 percent can change the sound velocity by almost a factor of two.

Helium films on alkali metal substrates have recently received much attention because of the discovery of non-wetting of ^{4}He in cesium.[32–34] The possibility of "non-wetting" or "pre-wetting" of ^{4}He on weakly attractive substrates has been implicit to theoretical calculations for quite some time, c.f. Ref. 35, Table III, Ref. 36, and more recently in Ref. 37. As pointed out in Ref. 21, the generic phenomenon has actually little to do with the *many-body* aspects of helium films. An argument similar to the qualitative discussions of Refs. 21 and 38 illustrates the situation: The simplest criterion whether a *low-coverage* ^{4}He film would wet, at $T=0$, a substrate or not is whether it is energetically more favorable for a single atom to be adsorbed to the substrate, or to a droplet of liquid helium. Thus, roughly, when the binding energy of the single particle to the substrate is *greater* than the chemical potential of an atom in the bulk liquid, the film would wet, otherwise it will not. This picture *assumes*, of course, that the chemical potential is a reasonably smooth function of the surface coverage. While it is not guaranteed that the chemical potential is rigorously monotonic, especially for thin films (see our discussion above and also the results of Ref. 21) this picture describes the overall features quite well. In other words, *any theory* that reduces to the one-body Schrödinger equation for the single particle in the limit of infinitesimal particle number, and reproduces (or fits) the bulk chemical potential should make reasonable predictions of the wetting behavior of the liquid. Many-particle effects become relevant only when one studies the deviation from these two limits. In this aspect, the HNC/EL theory and the NLDFT make rather different predictions.

The alkali metal substrate potentials are interesting since the layering transitions are less pronounced than on the graphite/solid helium potential. We have calculated the structure of ^{4}He films on alkali metal substrates starting from the lowest stable coverage up to a coverage of $n=0.24$ Å^{-2}, which corresponds, for a magnesium substrate, to slightly more than three layers. Figs. 8 show, for the purpose of further discussion, the corresponding density profiles. Fig. 9 shows the chemical potential, as a function of coverage, for the three substrate potentials corresponding to Mg, Li, and Na, and a comparison with the results of the NLDFT. In all cases, the HNC/EL calculations predict the expected oscillations and a minimum

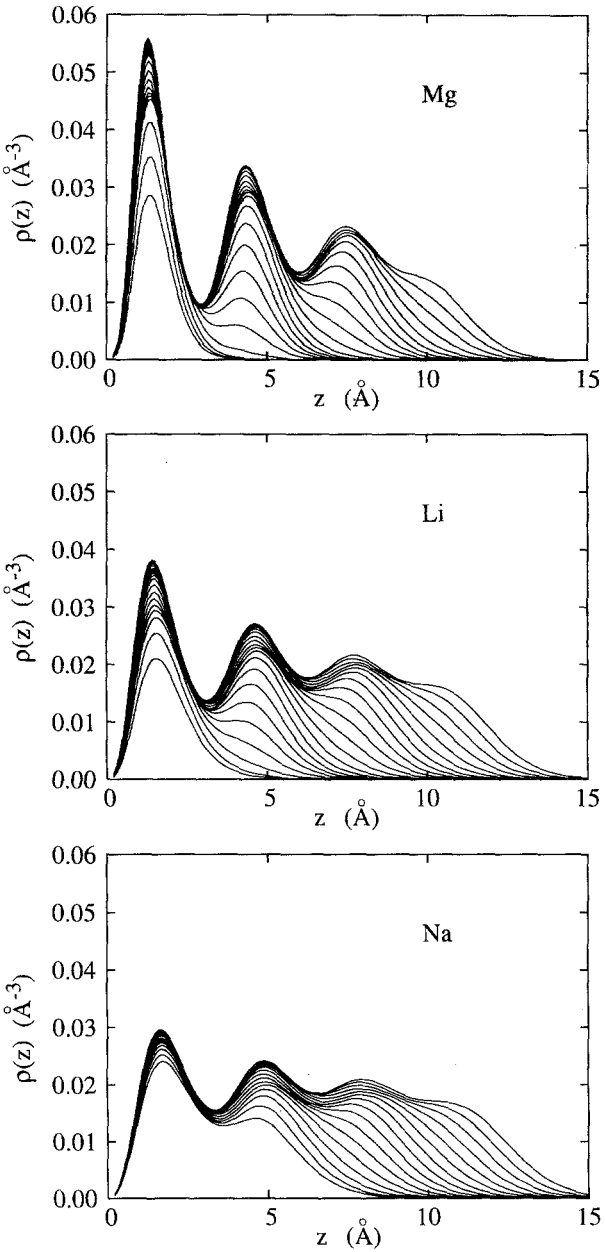

Fig. 8. The density profiles of ^{4}He films adsorbed to the alkali metal substrates as obtained from the HNC/EL theory. The curves correspond to coverages of $n = 0.04$ Å$^{-2} \cdots 0.24$ Å^{-2} for Mg and Li, and to $n = 0.09$ Å$^{-2} \cdots 0.24$ Å^{-2} for Na.

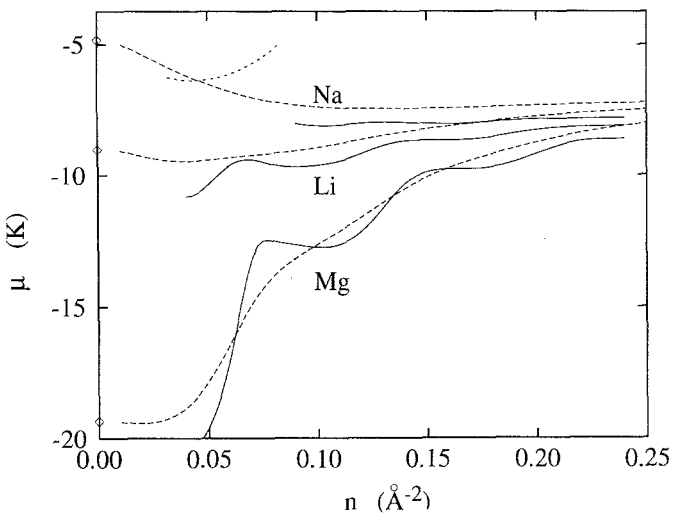

Fig. 9. The chemical potentials of ^{4}He films adsorbed to the substrates Mg (lowest solid line), Li (middle solid line) and Na (highest solid line) as obtained from the HNC/EL theory and from the NLDFT (dashed lines, same sequence). Also shown are the binding energies of a *single* helium atom to the substrate (diamonds at the left margin) and the chemical potential for a ^{4}He monolayer on a sodium substrate calculated by Carraro and Cole[38] (short-dashed line).

stable coverage. The fact that most of the instabilities found for the alkali metal substrates are so weak (mc_3^2 is of the order of -0.1 to -0.5 K at the minimum) means that one should not take these results as being completely conclusive.

Both the magnesium and the lithium substrates support a monolayer of sufficient coverage, but in both systems this monolayer is already rather "soft" in the sense that the chemical potential deviates, as a function of coverage, significantly from the two-dimensional estimate (5.8). This finding is consistent with our estimate that the single helium atom must be bound stronger to the substrate than to the bulk helium to have wetting. These binding energies are 19.35 K for Mg and 9.01 K for Li.

In Na, we do *not* find monolayer solutions, the lowest stable coverage is 0.1 Å^{-2}, or about two layers; only by projecting out the very long-wavelengths excitations we were able to extend the calculations to a coverage of 0.09 Å^{-2}. This observation implies that, in the early stages of the growth of helium films on Na, the helium atoms form bulk-like clusters, at least two atoms thick in the third dimension. Above a coverage of about 0.09 Å^{-2}, the clusters are fully connected such that the helium uniformly covers the surface. These results are similar to those of Cheng *et al.*[21]

obtained in NLDFT, whose minimum stable coverage is, being derived from a more repulsive equation of state, slightly larger than ours. The similarity of the results of Ref. 21 and ours is yet another confirmation of our assessment that the global adsorption scenario has very little to do with many body physics, but only the detailed structure of the adsorbate.

This is consistent with the fact that the binding energy of the single atom to the substrate is, with -4.83 K significantly less than the chemical potential of the bulk liquid. Indeed, Na is a borderline case where the chemical potential is almost flat as a function of coverage n; in the coverage regime considered here it increases only by about 0.1 K. While the oscillations of the chemical potential and the speed of sound are still systematic as a function of coverage, they are so small that we cannot make a reliable estimate for their amplitude.

Globally, our theoretical results are in agreement with the observation by Nacher and Dupont-Roc[33] who found that ^{4}He wets a Na surface. On the microscopic scale, one would, however, conclude that the minimum stable coverage is a double layer and not, as on stronger substrates, a monolayer. Such an effect might be detectable in torsion-oscillator experiments of the kind reported by Crowell and Reppy[6] since one would be lead to the conclusion that the minimum coverage where superfluidity appears is more than a monolayer.

The asymptotic value of the chemical potential also gives some estimate for the numerical accuracy of our calculations. The largest uncertainty arises because in the evaluation of the "elementary diagrams," which involve, when done exactly, the calculation of a function of three variables (z_1, z_2, and $r_{||}$), where each function value is a six-dimensional integral. To simplify this calculation, we have used a "spherically averaged" pair distribution funtion and evaluated the integrals at an average density. This causes apparently a small overestimate of the chemical potential of about 0.5–0.6 K in the asymptotic bulk limit. Since the behavior of our films is basically dominated by the difference between the structure at *neighboring* coverages, this inaccuracy will not in any way seriously affect our conclusions. Of course, with Na being a borderline case, these results should be taken with some caution and must await confirmation by a more accurate theory. For that reason, we have not attempted to carry out calculations for the even weaker substrate potentials for K, Rb, and Cs.

On a somewhat more technical level, our studies allow for an interesting comparison with a calculation of the energetics of a ^{4}He monolayer on a Na substrate by Carraro and Cole.[38] These authors have carried out variational Monte Carlo calculation, using a Schiff-Verlet type parametrized correlation function of the form $u_2(\mathbf{r}_i, \mathbf{r}_j) = -(b/|\mathbf{r}_i - \mathbf{r}_j|)^m$. For the *given correlation function*, the calculation is exact. Our energy evaluation is,

on the other hand, approximate, but the correlation function has the most general form permitted by the symmetry of the problem. The difference between our results and those by Carraro and Cole is striking: our calculations indicate that the minimum stable coverage of ^{4}He on sodium would be two layers, or $n \approx 0.1$ Å^{-2}. Carraro and Cole report that an atomic monolayer can be stable at a saturation surface coverage of $n \approx 0.062$ Å^{-2}. The dramatic *qualitative* difference between the predictions of the variational Monte Carlo calculation and our optimized HNC calculation is, to our knowledge, unprecedented in the history of quantum Monte Carlo calculations for the helium liquids.

Our *interpretation* of the discrepancy of the results is that the Schiff-Verlet wave function does not adequately describe the degree of freedom of particles moving in the direction perpendicular to the symmetry plane. In our earlier calculations of Ref. 7, (and also in the calculations on the magnesium substrate) we found that the correlations and the nature of the excitation modes changes abruptly and radically shortly before a layer becomes unstable against the promotion of particles to the next higher layer. The effect is particularly pronounced for a high-coverage monolayer. The analytic properties of the optimal pair correlation function become in this case quite different,[39] and it would not be surprising if the Schiff-Verlet functions do not well represent this effect.

If our interpretation is correct, one is led to suspect that an "educated guess" for a variational wave function, to be used in Monte Carlo calculations, can be quite misleading. Of course, a definite answer can be obtained only by a calculation that supercedes both the Carraro-Cole calculation and ours in quality, i.e., a Green's function Monte Carlo (GFMC)[40] or a diffusion Monte Carlo (DMC)[41] calculation.

6. DYNAMIC STRUCTURE FUNCTION

We have shown in previous work[8,20] how the solutions of Eq. (2.7) can be used to construct the dynamic structure function in an approximation equivalent to the Feynman theory for the collective excitation energies. The Feynman theory can be interpreted in terms of a linear response theory with a *local* particle-hole interaction. The density-density response function is given in the random-phase approximation (RPA) by the relation

$$\chi(\mathbf{r}_1, \mathbf{r}_2; \omega) = \chi_0(\mathbf{r}_1, \mathbf{r}_2; \omega) + \int d^3r_3\, d^3r_4\, \chi_0(\mathbf{r}_1, \mathbf{r}_3; \omega) \times V_{\text{p-h}}(\mathbf{r}_3, \mathbf{r}_4)\, \chi(\mathbf{r}_4, \mathbf{r}_2; \omega) \tag{6.1}$$

where $\chi_0(\mathbf{r}_1, \mathbf{r}_2; \omega)$ is the response function of a "non-interacting" system defined by the one-body Hamiltonian H_1:

$$\chi_0(\mathbf{r}_1, \mathbf{r}_2; \omega) = 2\sqrt{\rho_1(\mathbf{r}_1)}\, H_1[(\hbar\omega)^2 - H_1^2 + i\eta]^{-1}\sqrt{\rho_1(\mathbf{r}_2)} \tag{6.2}$$

and $V_{\text{p-h}}(\mathbf{r}, \mathbf{r}')$ is the "particle-hole interaction". The HNC theory provides a specific expression for this effective interaction, but, as pointed out above, the NLDFT can alternatively be used in Eq. (2.12) to obtain a static effective interaction for the linear response Eq. (6.1).

Using the representation (6.2) of $\chi_0(\mathbf{r}, \mathbf{r}'; \omega)$, one can formally solve for the full response function $\chi(\mathbf{r}, \mathbf{r}'; \omega)$:

$$\begin{aligned}\chi(\mathbf{r}, \mathbf{r}'; \omega) &= 2\sqrt{\rho_1(\mathbf{r})}\,\{[(\hbar\omega)^2 - H_1^2 - 2H_1\hat{V}_{\text{p-h}} + i\eta]^{-1} H_1\}\sqrt{\rho_1(\mathbf{r}')} \\ &= 2\sum_{\omega'}\sqrt{\rho_1(\mathbf{r})}\,\phi_{\omega'}(\mathbf{r})\frac{1}{(\hbar\omega)^2 - (\hbar\omega')^2 + i\eta}\phi_{\omega'}(\mathbf{r}')\sqrt{\rho_1(\mathbf{r}')}\end{aligned} \tag{6.3}$$

where $\phi_{\omega'}(\mathbf{r})$ and the $\hbar\omega'$ are the eigenfunctions and eigenvalues of

$$\int d^3r'\, H_1(\mathbf{r})[\delta(\mathbf{r} - \mathbf{r}')\, H_1(\mathbf{r}') + 2\tilde{V}_{\text{p-h}}(\mathbf{r}, \mathbf{r}')]\,\phi_\omega(\mathbf{r}') = (\hbar\omega)^2\,\phi_\omega(\mathbf{r}). \tag{6.4}$$

Eq. (6.4) is the adjoint of the Euler Eq. (2.7). This analysis justifies identifying the eigenvalues of Eq. (2.7) with the collective modes of the system and, the (adjoint) eigenfunctions with the transition densities corresponding to the individual excitation modes,

$$\delta\rho_\omega(\mathbf{r}) = \sqrt{\rho_1(\mathbf{r})}\,\phi_\omega(\mathbf{r}). \tag{6.5}$$

From the density-density response function (6.3) one obtains finally the dynamic structure function

$$\begin{aligned}S(\mathbf{r}, \mathbf{r}'; \omega) &= -\frac{1}{\pi}\,\text{Im}\,\chi(\mathbf{r}, \mathbf{r}'; \omega) = \sqrt{\rho_1(\mathbf{r})}\,\phi_\omega(\mathbf{r})\,\phi_\omega(\mathbf{r}')\sqrt{\rho_1(\mathbf{r}')} \\ &= \delta\rho_\omega(\mathbf{r})\,\delta\rho_\omega(\mathbf{r}').\end{aligned} \tag{6.6}$$

In our geometry, the dynamic structure function is diagonal in the momentum $\mathbf{q}_{||}$ parallel to the surface. The spectrum of excitation energies $\hbar\omega$ is discrete for energies smaller than the separation energy, i.e. for

$$\hbar\omega + \mu < \hbar^2 q_{||}^2/2m, \tag{6.7}$$

otherwise it is continuous. Most scattering experiments have been performed at grazing angles and we therefore consider only momenta parallel

to the surface. Thus, we define the *diagonal* dynamic structure function in momentum space

$$S(q_{||};\omega) = \int dz\, dz'\, d^2r_{||}\, e^{i\mathbf{q}_{||}\cdot\mathbf{r}_{||}} \sqrt{\rho_1(\mathbf{r})}\, S(\mathbf{r},\mathbf{r}';\omega) \sqrt{\rho_1(\mathbf{r}')}$$
$$= |\delta\rho_\omega(q_{||})|^2 \tag{6.8}$$

where

$$\delta\rho_\omega(q_{||}) = \int dz\, \delta\rho_\omega(z, q_{||}) = \int dz \sqrt{\rho_1(z)}\, \phi_\omega(z, q_{||}) \tag{6.9}$$

are the *transition densities* corresponding to the excitation of frequency ω and parallel momentum $\mathbf{q}_{||}$.

The Feynman theory has it's well-known deficiencies but within the HNC/EL theory, a systematic path for improvement is to allow for a time-dependence of the pair correlation functions appearing in the variational wave function (2.1) and to solve a linearized set of equations of motion for the time-dependent component.[27,28] We have recently implemented this strategy[42,9,43,44] and shown that, within certain approximations, the equations of motion method leads to the same Brillouin-Wigner type perturbation formula as the correlated-basis-functions theory of Chang and Campbell.[26] An important result of these studies is that the improved theory produces a significant shift of the excitation spectrum to lower energies, but has little effect on the overall physical picture. The generalized Brillouin-Wigner theory in the non-uniform geometry is numerically quite demanding and no neutron scattering data are available for alkali metal substrates which are the main focus of this paper. We therefore restrict ourselves here to the Feynman approximation which is sufficient to highlight the difference between excitation spectra on weakly and strongly attractive substrates and between the two different theories discussed here.

When the eigenvalue Eq. (2.7) is discretized on a finite mesh, only the discrete subset of the continuum states is obtained that corresponds to excitation functions which vanish at the boundary of the discretization box. In such an approximation, the resulting $S(q_{||};\omega)$ is a series of δ-functions,

$$S(q_{||};\omega) \approx \sum_n |\delta\rho_\omega(q_{||})|^2\, \delta(\omega - \omega_n) \tag{6.10}$$

However, all functions appearing in the kernel of Eq. (2.7) can be easily extrapolated to their asymptotic values for large distances from the surface. One can therefore extend the mesh to large distances to obtain a very dense spectrum from which reliable information on the density of

states can be extracted. We have typically discretized the eigenvalue problem (2.7) in a box of 50 Å as compared to our film thickness of about 10–15 Å.

Maps of dynamic structure functions for a sequence of coverages on Mg and Na substrates are shown in Figs. 10 and 11. These two sets of figures cover a reasonably wide range of coverages and potential strengths.

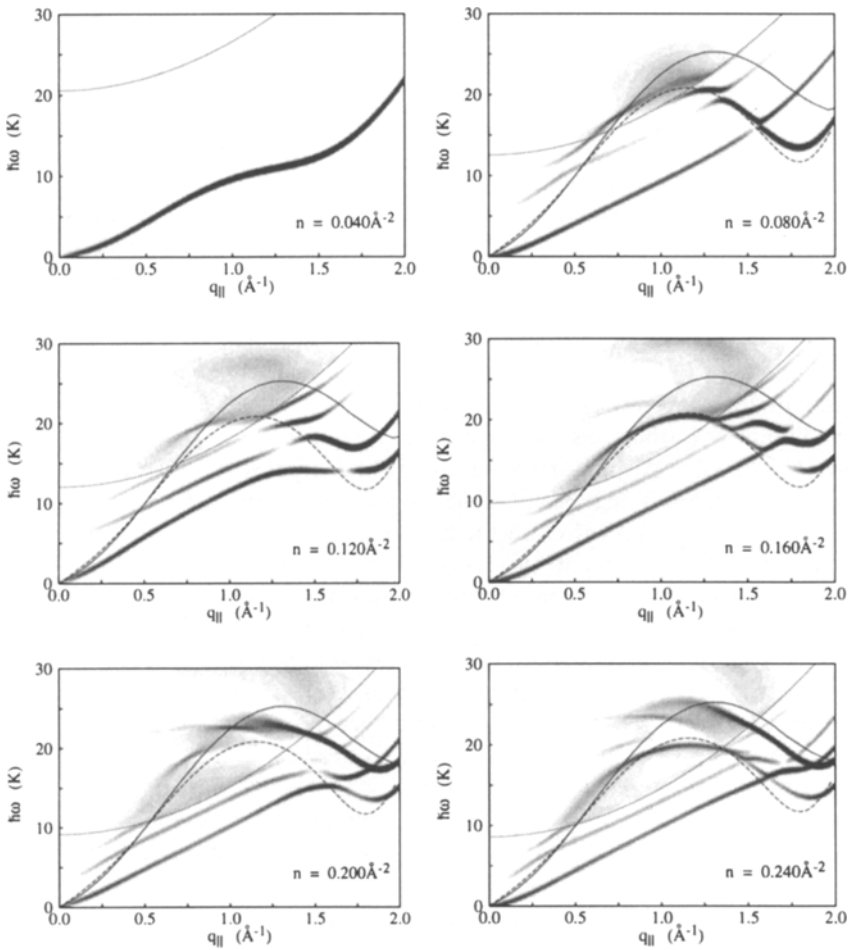

Fig. 10. The dynamic structure function $S(q_{||}; \omega)$, obtained from the HNC/EL theory, is shown, in Feynman approximation, for a representative sample of films on a magnesium substrate. The grayscale indicates the strength of $S(q_{||}; \omega)$. The dotted parabolic line in the middle of the frames is the boundary of continuum states, the solid line is the Feynman spectrum of the *three-dimensional* bulk liquid at $\rho = 0.022\ \text{Å}^{-3}$, and the dashed line the Feynman spectrum of the *two-dimensional* bulk liquid at $n = 0.065\ \text{Å}^{-2}$.

The figures show also, for reference, the continuum boundary $\hbar\omega + \mu < \hbar^2 q_{||}^2/2m$. All modes *below* this continuum boundary are discrete in Feynman approximation; in order to display their relative strength we have artificially broadened these δ-function states by replacing them with Gaussians of approximately 0.5 K width:

$$S(q_{||}; \omega) \approx \sum_n |\delta\rho_\omega(q_{||})|^2 \frac{1}{\varepsilon\sqrt{\pi}} \exp\left[-\left(\frac{\omega - \omega_n}{\varepsilon}\right)^2\right] \tag{6.11}$$

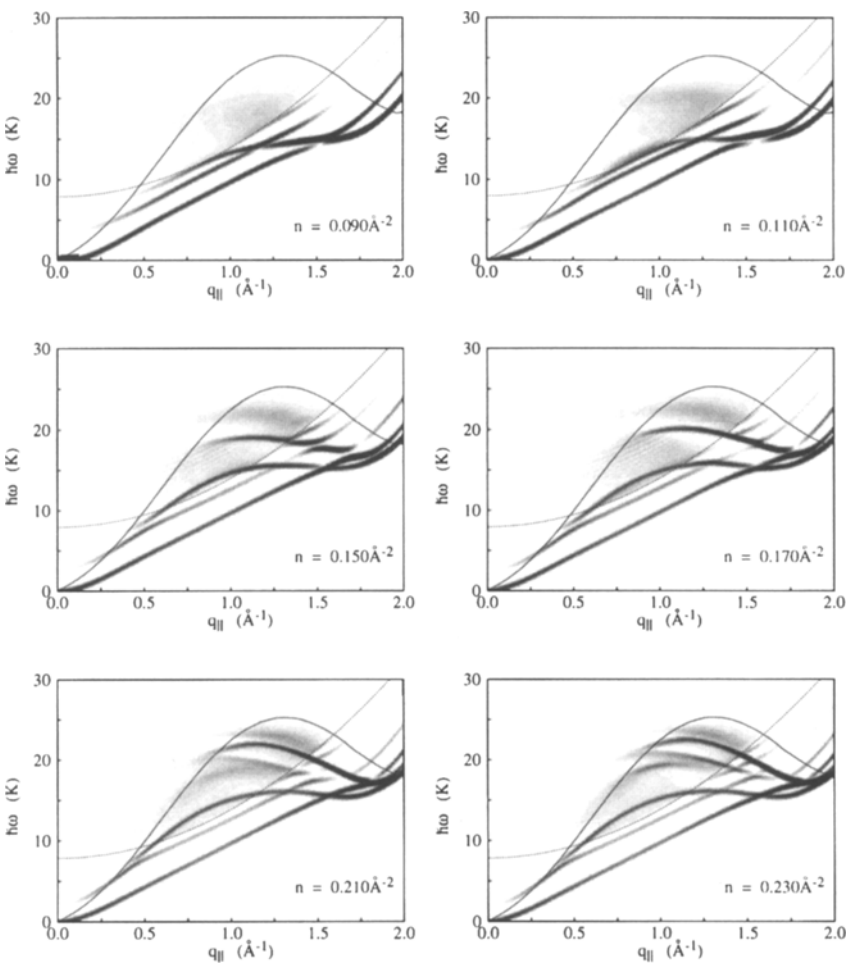

Fig. 11. Same as Fig. 10 for helium films on a Na substrate. The Feynman spectrum of the *two-dimensional* bulk liquid has been omitted.

The figures also show the Feynman dispersion relations of the three-dimensional liquid and, for the Mg films with coverage $n \geq 0.080$ Å^{-2}, the dispersion relation of the two-dimensional liquid corresponding to an areal density of $n = 0.065$ Å^{-2}. This coverage is near the solidification density of the two-dimensional superfluid. For the lowest coverage monolayer film with $n = 0.040$ Å^{-2}, the dispersion relation of the film and the one of the two-dimensional liquid with the same areal density are practically indistinguishable.

The number of excitation modes increases with coverage, and the $S(q_{||}; \omega)$ gains strength (as indicated by the grayscale) along a path, through several individual "modes," in the $(q_{||}; \omega)$ plane, which resembles the three-dimensional bulk phonon-roton spectrum. A second rather clear strength distribution pattern is found in Mg films with $n \geq 0.080$ Å^{-2} in the "maxon-roton" region along the dispersion relation of the *two-dimensional* fluid. This strength distribution agrees best with a two-dimensional phonon-roton spectrum corresponding to an areal density of $n = 0.065$ Å^{-2}. This areal density is *somewhat less* than the amount of material contained in the first layer, which corresponds to a coverage of approximately $n = 0.075$ Å^{-2}. This mode corresponds, as we will show more explicitly below, to the propagation of the excitation within the first liquid layer. A strong third mode is found well below those two phonon branches. We identify this mode with the ripplon. The two weaker modes parallel to the ripplon mode are remnants of two bound excited states of the Mg substrate potential perpendicular to the surface. In the infinitesimal coverage limit their binding energies are 6.02 K and 1.42 K. Starting with a coverage of $n = 0.080$ Å^{-2}, the maps of $S(q_{||}; \omega)$ show clearly the phenomenon of at least two level crossings where the two-dimensional phonon crosses the ripplon modes. The number of crossings is doubled when the second layer becomes filled at $n = 0.160$ Å^{-2} and the three-dimensional bulk-like mode begins to gain strength at the expense of the two-dimensional mode.

A clear identification of the nature of the individual excitations is obtained by considering the *transition densities* $\delta\rho_1(z, q_{||})$. These are shown, for the *energetically lowest excitations* in the Mg film with $n = 0.240$ Å^{-2}, in Fig. 12. Indeed, up to a wave number $q_{||} \approx 1.6$ Å^{-1}, the lowest-lying excitation qualifies as a surface mode. The nature of the excitation changes abruptly, for a small momentum regime 1.6 Å$^{-1} < q_{||} < 1.8$ Å^{-1} there appears to be a resonance between the two first layers. But at wave numbers $q_{||} > 1.8$ Å^{-1}, the wave propagates mainly in the first layer.

The situation is not so clear in the Na films in the sense that there is no mode that can be identified unambiguously as the one propagating in the first liquid layer. This is plausible since the layer structure is much less pronounced (c.f. Fig. 8), in particular there exists no stable monolayer. We

see, of course, still the expected surface mode and a weaker parallel mode due to one bound excited state of the Na substrate potential. In the limit of one helium atom on the surface the excited state is bound only by 0.77 K. As the coverage is increased, the film approaches the bulk limit somewhat more slowly, but still quite visibly. Hence, the bulk maxon-roton spectrum is somewhat less pronounced at the coverages under consideration here.

We have also used the effective interation as derived via Eq. (2.12) from the NLDFT. Two representative maps of $S(q_{||}; \omega)$ are shown in Fig. 13. After the discussions of the energetics and the structure functions in the bulk two- and three-dimensional cases, the results are hardly sur-

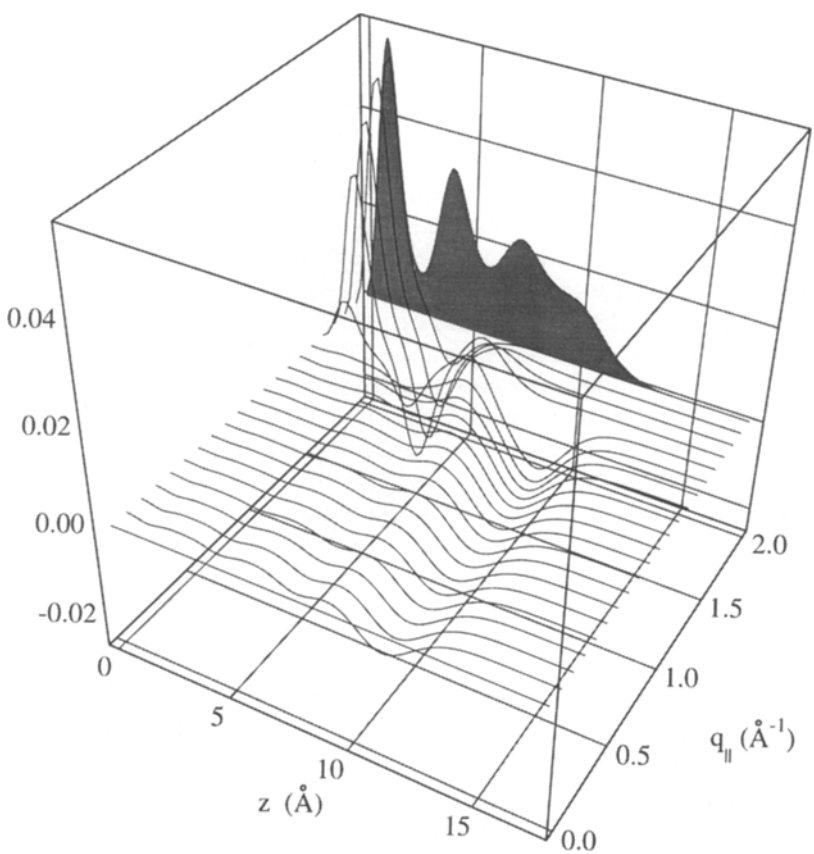

Fig. 12. Transition densities of the lowest excited state of a multilayer ^{4}He films with areal densities of $n = 0.24$ Å^{-2} on a Mg substrate. The shaded area in the background is the ground state profile, the individual lines are the transition densities $\delta\rho_1(z, q_{||})$ in steps $\Delta q_{||} = 0.1$ Å^{-1}.

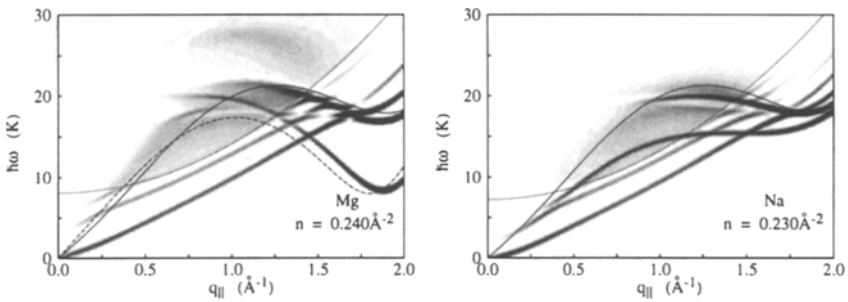

Fig. 13. Same as Figs. 10 and 11 as calculated from the NLDFT. Note that the Feynman spectra of both the three- and the two-dimensional bulk liquid have also been calculated using the NLDFT. Note that the two-dimensional phonon corresponds to an areal density of $n = 0.07$ Å^{-2}, whereas the first layer has, within that theory, an areal density between 0.08 Å^{-2} and 0.085 Å^{-2}.

prising: Consistent with our findings for the HNC/EL case, we find in both films a maxon-roton excitation which follows quite closely the maxon-roton branch of the bulk three-dimensional calculation *within the same theory*. Consistent with the lacking structure of the three-dimensional NLDFT $S(q)$, the maxon comes out to be somewhat too flat. We also find, for the Mg substrate, a "two-dimensional" maxon-roton branch which is roughly consistent with the predictions of that theory in two dimensions. As suggested by the shape of the structure functions shown in Fig. 3, the "roton minimum" predicted by the NLDFT is much too low for a Feynman theory. Note that the two-dimensional dispersion relation shown in Fig. 13 corresponds to a surface coverage of $n = 0.07$ Å^{-2}, whereas the first layer on the Mg substrate corresponds to a surface coverage of roughly $n = 0.08$ Å^{-2}. At that areal density, the bulk NLDFT predicts, in two dimensions, an instability at *finite* wave numbers, i.e. the energy spectrum $\hbar\omega$ of Eq. (4.6) becomes imaginary. In summary, the theory leads to *qualitatively similar* conclusions on the nature of the film excitations as the microscopic HNC/EL theory, but it has quantitative deficiencies.

7. SUMMARY

We have in this paper extended our calculations of Ref. 7 to the case of alkali metal substrates, and have carried out a comparison with the predictions of the non-local density-functional theory proposed in Refs. 10, 21. We have tried to be conservative with our predictions and have compared, wherever available, with independent Monte Carlo calculations and/or experiments. All of our tests have turned out to be quite satisfactory. It would nevertheless be extremely useful to have a few benchmark calcula-

tions to verify the energetics of adsorbed films, in particular in the region of our predicted layering phase transitions.

Our calculations have been spawned by the experimental discovery of non-wetting of ^{4}He on some alkali metal substrates.[32–34] We have argued above that a first estimate of the wetting behavior at $T=0$ can be obtained by comparing the binding energy of a single atom to the substrate to the chemical potential of that atom in the liquid. In other words, the wetting behavior is, to first approximation, *not a many-body phenomenon.* Our results have confirmed this, as well as the fact that the *details* of the wetting scenario (e.g. the minimum number of stable layers) are determined by very subtle many-body effects. Only at that level, many-body effects are relevant, and the predictions of the microscopic HNC/EL theory and the NLDFT are very different.

As pointed out above, the HNC/EL equations have no solutions if the assumed geometry is unstable under infinitesimal density fluctuations. This is a desirable feature of the theory, and evidently of particular relevance in the wetting problem. Of course, this feature makes the theory considerably harder to use than, for example, a mean-field theory since the convergence of the calculations becomes very delicate in the vicinity of an instability. We have therefore not tried to weaken the strength of our substrate potential below the strength of Na and use alkali metal substates like Cs and Rb. The chemical potential of Na for the stable coverages of more than two layers is already essentially flat and we believe that the results with weaker substrate potentials would be beyond the predictive power of the HNC/EL theory (or, for that matter *any* other theory available now.)

As a general feature, we found that the sound velocity is an extremely ensitive function of the substrate potential. In keeping with our cautious assessment of present-days theoretical models, we feel that we are presently perhaps capable of predicting energies and chemical potentials within an accuracy of a few percent. But the calculation of sound velocities is more difficult and also plagued by intrinsic difficulties of microscopic theories as mentioned below Eq. (5.3). The reader interested in these technical details is referred to Ref. 16 for a discussion of this subtle point. We feel that there are sufficiently large uncertainties in the substrate potentials to allow for an assessment whether or not a theory predicts the "correct" sound velocity.

We have also carried out a comparison between the results of the HNC/EL theory and the NLDFT recently used extensively by Pavloff and Treiner[10] and by Cheng *et al.*[21] The important points have been made in the body of this paper, we only need to summarize our findings. The main problem of the NLDFT is that it does not reproduce well the two-dimensional equation of state. While it was not *a priori* clear that this is a relevant concern, we have shown here and elsewhere[7] that a low to medium

coverage atomic monolayer is indeed reasonably well approximated by a two-dimensional system. The essential difference is that the HNC/EL theory (as well as exact Monte Carlo integrations) predict that the two-dimensional system is bound, whereas the NLDFT predicts an insignificant binding. In this respect, the NLDFT is plagued by the same problem as our earlier HNC calculations[35] which omitted triplet correlations and therefore also missed much of the binding of the two-dimensional system, leading to less pronounced layer structures and weaker oscillations in the sound velocity.

NOTE ADDED IN PROOF

Our chemical potential in the two-dimensional limit of the NLDFT shown in Fig. 1 deviates somewhat from the value $\mu = -0.18$ K at $\rho_{2D} = 0.026$ Å^{-2} given in Ref. 21. This discrepancy has in the meantime be clarified (M. W. Cole, private communication). After this paper was submitted, a path integral monte carlo simulation of ^{4}He on a solid hydrogen substrate was published (M. Wagner and D. Ceperley, *J. Low Temp. Phys.* **94**, 185 (1994)). This work comes to conclusions similar to ours on a layering transition of ^{4}He on sufficiently strong substrates. The discussion at the end of Section 5 has to be seen in view of this new evidence supporting our scenario.

ACKNOWLEDGMENTS

The work was supported, in part, by the North Atlantic Treaty Organization under a Grant awarded in 1992 (to B. E. C.), the National Science Foundation under grants PHY-9108066 and INT-9014040 (to E. K.), and the Academy of Finland (to M. S.), B. E. C. is grateful to Nordita for supporting his visit to the University of Oulu where part of the work was done. Discussions with M. Cole and J. Treiner are gratefully acknowledged.

REFERENCES

1. M. J. McKenna, T. B. Brosius, and J. D. Maynard, *Phys. Rev. Lett.* **69**, 3346 (1992).
2. B. E. Clements, E. Krotscheck, and H. J. Lauter, *Phys. Rev. Lett.* **70**, 1287 (1993).
3. H. J. Lauter, H. Godfrin, V. L. P. Frank, and P. Leiderer, in *Excitations in Two-Dimensional and Three-Dimensional Quantum Fluids, Vol. 257 of NATO Advanced Study Institute, Series B: Physics*, A. F. G. Wyatt and H. J. Lauter, eds. (Plenum, New York, 1991), p. 419.
4. H. J. Lauter, H. Godfrin, V. L. P. Frank, and P. Leiderer, *Phys. Rev. Lett.* **68**, 2484 (1992).
5. D. S. Greywall and P. A. Busch, *Phys. Rev. Lett.* **67**, 3535 (1991).
6. P. A. Crowell and J. D. Reppy, *Phys. Rev. Lett.* **70**, 3291 (1993).

7. B. E. Clements, J. L. Epstein, E. Krotscheck, and M. Saarela, *Phys. Rev. B* **48**, 7450 (1993).
8. E. Krotscheck and C. J. Tymczak, *Phys. Rev. B* **45**, 217 (1992).
9. B. E. Clements, E. Krotscheck, H. J. Lauter, and M. Saarela, in *Condensed Matter Theories*, J. W. Clark, A. Sadiq, and K. A. Shoaib, eds. (Nova Science Publishers, Commack, NY, 1994), Vol. 9.
10. N. Pavloff and J. Treiner, *J. Low Temp. Phys.* **83**, 331 (1991).
11. J. Dupont-Roc, M. Himbert, N. Pavloff, and J. Treiner, *J. Low Temp. Phys.* **81**, 31 (1990).
12. G. Baym and L. P. Kadanoff, *Phys. Rev.* **124**, 287 (1961).
13. A. D. Jackson, A. Lande, and R. A. Smith, *Phys. Rep.* **86**, 55 (1982).
14. A. D. Jackson, A. Lande, and R. A. Smith, *Phys. Rev. Lett.* **54**, 1469 (1985), and references therein.
15. E. Krotscheck, Q.-X. Qian, and W. Kohn, *Phys. Rev. B* **31**, 4245 (1985).
16. E. Krotscheck and M. Saarela, *Phys. Rep.* **232**, 1 (1993).
17. E. Krotscheck, *Phys. Rev. B* **31**, 4258 (1985).
18. C. Ji and M. Wortis, *Phys. Rev. B* **34**, 7704 (1986).
19. P. Leiderer, *J. Low Temp. Phys.* **87**, 247 (1992).
20. S. A. Chin and E. Krotscheck, *Phys. Rev. B* **45**, 852 (1992).
21. E. Cheng, M. W. Cole, W. F. Saam, and J. Treiner, *Phys. Rev. B* **46**, 13967 (1992).
22. R. de Bruyn Ouboter and C. N. Yang, *Physica* **144B**, 127 (1986).
23. M. H. Kalos, M. A. Lee, P. A. Whitlock, and G. Chester, *Phys. Rev. B* **24**, 115 (1981).
24. P. A. Whitlock, G. V. Chester, and M. H. Kalos, *Phys. Rev. B* **38**, 2418 (1988).
25. S. Stringari and J. Treiner, *J. Chem. Phys.* **87**, 5021 (1987).
26. C. C. Chang and C. E. Campbell, *Phys. Rev. B* **13**, 3779 (1976).
27. M. Saarela, *Phys. Rev. B* **33**, 4596 (1986).
28. M. Saarela and J. Suominen, in *Condensed Matter Theories*, J. S. Arponen, R. F. Bishop, and M. Manninen, eds. (Plenum, New York, 1988), Vol. 3, p. 157.
29. E. C. Svensson, V. F. Sears, A. D. B. Woods, and P. Martel, *Phys. Rev. B* **21**, 3638 (1980).
30. H. N. Robkoff and R. B. Hallock, *Phys. Rev. B* **24**, 159 (1981).
31. M. W. Cole, D. R. Frankl, and D. L. Goodstein, *Rev. Mod. Phys.* **53**, 199 (1981).
32. K. S. Ketola, S. Wang, and R. B. Hallock, *Phys. Rev. Lett.* **68**, 201 (1992).
33. P. J. Nacher and J. Dupont-Roc, *Phys. Rev. Lett.* **67**, 2966 (1991).
34. J. Rutlege and P. Taborek, *Phys. Rev. Lett.* **68**, 2184 (1992).
35. E. Krotscheck, *Phys. Rev. B* **32**, 5713 (1985).
36. J. L. Epstein and E. Krotscheck, *Phys. Rev. B* **37**, 1666 (1988).
37. E. Cheng, M. Cole, W. Saam, and J. Treiner, *Phys. Rev. Lett.* **67**, 1007 (1991).
38. C. Carraro and M. W. Cole, *Phys. Rev. B* **46**, 10947 (1992).
39. B. E. Clements, E. Krotscheck, and M. Saarela, *Z. Physik* (1994), in press.
40. M. A. Lee, K. E. Schmidt, M. H. Kalos, and G. V. Chester, *Phys. Rev. Lett.* **44**, 728 (1981).
41. S. A. Chin, *Phys. Rev. A* **42**, 6991 (1990).
42. B. E. Clements *et al.*, *J. Low Temp. Phys.* **89**, 585 (1992).
43. B. E. Clements *et al.*, *Phys. Rev. B* (1994), (to be published).
44. B. E. Clements *et al.*, in *XX International Conference on Low Temperature Physics, Conference Handbook*, R. J. Donelly, ed. (University of Oregon, Oregon, 1993), pp. Abstract J5-8.